



ELSEVIER

Journal of Non-Crystalline Solids 265 (2000) 75–82

JOURNAL OF  
NON-CRYSTALLINE SOLIDS

www.elsevier.com/locate/jnoncrystal

# Relationships between bridging oxygen $^{17}\text{O}$ quadrupolar coupling parameters and structure in germanates

Ted M. Clark, Philip J. Grandinetti \*

*Department of Chemistry, The Ohio State University, 120 W. 18th Avenue, Columbus, OH 43210-1173, USA*

Received 1 June 1999; received in revised form 7 October 1999

## Abstract

We have performed ab initio calculations on the model cluster  $(\text{OH})_3\text{Ge}-\text{O}-\text{Ge}(\text{OH})_3$  in order to refine the relationships between  $^{17}\text{O}$  quadrupolar coupling parameters and the local structure around the bridging oxygen. From these calculations the trend in the bridging oxygen  $^{17}\text{O}$  quadrupolar coupling constant,  $C_q$ , and asymmetry parameter,  $\eta_q$ , with changing Ge–O–Ge angle was found to be similar to previously established trends in silicate clusters with the overall  $C_q$  values being systematically increased in magnitude by approximately 3 MHz. Such a shift can be attributed to differences in cation–oxygen distances as well as coordinating cation electronegativity. In addition, we also investigated the effect of changing intratetrahedron bond angles over a range that has been suggested to exist in germanate systems. While such variations in intratetrahedron bond angles lead to a small variation in  $C_q$ ,  $\eta_q$  remains relatively unaffected. In such cases,  $\eta_q$  can still be a reliable probe of Ge–O–Ge angle while  $C_q$  could serve as a probe of tetrahedron distortions. © 2000 Elsevier Science B.V. All rights reserved.

## 1. Introduction

With the recent development of solid-state nuclear magnetic resonance (NMR) techniques such as dynamic-angle spinning (DAS) [1,2] and multiple-quantum-magic-angle-spinning (MQMAS) [3], solid-state  $^{17}\text{O}$  NMR is becoming an increasingly useful technique for the probing of structure in solids, including glasses [4], polymers [5] and ceramic materials [6]. However, the inherent difficulties associated with  $^{17}\text{O}$  NMR in the past have precluded the establishment of well-defined relationships between  $^{17}\text{O}$  NMR parameters and structure which presently exist for

commonly used spin 1/2 probes such as  $^{13}\text{C}$  and  $^{29}\text{Si}$ . Ab initio calculations have assisted in establishing trends between  $^{17}\text{O}$  NMR parameters and structural features in crystalline silicates [7] and these derived theoretical trends have proven useful in the investigation of structural distributions in silicate glasses [4]. Also, application of molecular orbital calculations for the study of silicate model clusters such as  $(\text{OH})_3\text{Si}-\text{O}-\text{Si}(\text{OH})_3$  have supported the view that an understanding of bonding forces in representative molecules is useful for the modelling of structural features in chemically similar groups in solids [8]. The construction of 6-311 basis sets for third row atoms, including germanium [9], has allowed the theoretical study of germanate model clusters in an analogous manner to that completed for silicate model clusters [10]. Such a study is particularly relevant given the recent applications of

\* Corresponding author. Tel.: +1-614-292 6818; fax: +1-614-292 1685.

E-mail address: grandinetti.1@osu.edu (P.J. Grandinetti).

solid-state  $^{17}\text{O}$  NMR for studying the structure of germanate glasses and crystals [11,12].

The extension of ab initio calculations to representative model clusters containing germanium allows a comparison with ab initio results for silicon model clusters, as well as with experimental results for vitreous germanium oxide. In the present work these relationships are investigated and the correlation of NMR parameters with structural data for the germanate system is examined.

## 2. Theoretical

Ab initio calculations were performed using GAUSSIAN '94 [13] at a restricted Hartree-Fock level with 6-31 + G(*d*) and 6-311 + G(*d*) basis sets. GAUSSIAN '94 calculates the traceless electric field gradient (EFG) tensor and outputs its cartesian tensor elements. These calculated EFG tensor elements are related to the quadrupolar coupling constant,  $C_q$ , and quadrupolar coupling asymmetry parameter,  $\eta_q$ , according to

$$C_q = e^2 Q \langle q_{zz} \rangle / h, \quad \eta_q = \frac{\langle q_{xx} \rangle - \langle q_{yy} \rangle}{\langle q_{zz} \rangle}, \quad (1)$$

where  $e\langle q_{xx} \rangle$ ,  $e\langle q_{yy} \rangle$  and  $e\langle q_{zz} \rangle$  are the principal components of the electric field gradient tensor defined such that  $|\langle q_{zz} \rangle| > |\langle q_{yy} \rangle| > |\langle q_{xx} \rangle|$  and  $Q$  is the nuclear electric quadrupole moment. For  $^{17}\text{O}$  a value of  $e^2 Q / h = -6.11$  MHz a.u.<sup>3</sup> was used to convert the  $q_{zz}$  output from Gaussian into the  $^{17}\text{O}$  quadrupolar coupling constant. The sign of the quadrupolar constant was determined to be negative in all calculated cases.

The model cluster investigated in this paper was  $(\text{OH})_3\text{Ge}-\text{O}-\text{Ge}(\text{OH})_3$  and a graphical representation is shown in Fig. 1 with two possible

configurations, (a) staggered and (b) eclipsed. With variation of Ge–O–Ge and O–Ge–O bond angles, this cluster models the expected bridging oxygen environment in materials which include tetrahedrally coordinated germanium atoms, such as vitreous  $\text{GeO}_2$ .

When predicting the  $^{17}\text{O}$  quadrupolar coupling constant,  $C_q$ , there are two potential sources of error, that is,  $Q$  and  $q$ . For  $C_q$  calculations we use a value of  $Q$  determined experimentally for  $^{17}\text{O}$  to be  $Q = -2.6(\pm 0.1) \times 10^{-2}$  barns. Thus when comparing the magnitude of predicted  $C_q$  values with experiment we would expect an error on the order of 0.2 MHz due to uncertainty in  $Q$ .

There is also the contribution from inaccuracies in calculating the EFG. This affects both  $C_q$  and  $\eta_q$ , as seen by Eq. (1). The accepted approach is to assume that the true elements of the EFG tensor are related to the calculated elements according to

$$q_{ij}^{(\text{true})} = m q_{ij}^{(\text{calc})} + b,$$

using a common slope  $m$  and intercept  $b$ . In the case of EFG eigenvalues, however, one can show that  $b = 0$  since all the eigenvalues (including the calculated values) are constrained by  $q_{xx} + q_{yy} + q_{zz} = 0$ . Thus for the asymmetry parameter we find

$$\eta_q = \frac{m q_{xx} - m q_{yy}}{m q_{zz}} = \frac{m}{m} \left( \frac{q_{xx} - q_{yy}}{q_{zz}} \right) = \frac{q_{xx} - q_{yy}}{q_{zz}}$$

and see that  $\eta_q$  should be unaffected by the scaling. In general, the scaling factor  $m$  depends on the level of calculation employed. Finding the correct scaling factor for a given calculation requires comparison to experiment. In this ab initio study we find that the magnitude of  $C_q$  for a bridging oxygen in a germanate cluster is in close agreement

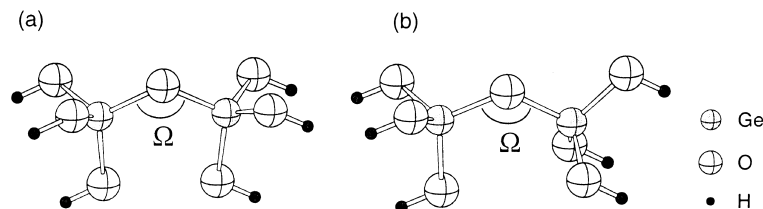


Fig. 1. Germanate model cluster  $(\text{OH})_3\text{Ge}-\text{O}-\text{Ge}(\text{OH})_3$  in (a) staggered and (b) eclipsed configurations.

with the value reported experimentally for  $\text{GeO}_2$  requiring a near unity scaling factor.

### 3. Results

The structure of amorphous  $\text{GeO}_2$  has been investigated by different experimental techniques, including EXAFS [14,15], Raman spectroscopy [16,17] and X-ray [18,19] and neutron diffraction [20,21]. The short-range structural order of both amorphous  $\text{GeO}_2$  and  $\text{SiO}_2$  under ambient conditions are similar and are based on the  $\alpha$ -quartz configuration of crystalline  $\text{GeO}_2$  and  $\text{SiO}_2$ , respectively. In both cases, bridging oxygen atoms link tetrahedrally coordinated germanium or silicon atoms with each oxygen atom having a coordination number of two.

The cluster  $(\text{OH})_3\text{Ge-O-Ge}(\text{OH})_3$  models the bridging oxygen environment present in amorphous  $\text{GeO}_2$  and calculated trends for this cluster may be compared with calculated results for analogous silicates [10]. The salient structural features of the germanate model cluster which may influence the quadrupole coupling parameters of the bridging oxygen atom that have been examined in this paper include (a) the angle  $\angle\text{O-Ge-OH}$ , (b) the placement of OH-groups, i.e. in either a staggered or eclipsed geometry, (c) the angle  $\angle\text{Ge-O-Ge}$  and (d) the Ge–O distance.

One manner in which amorphous  $\text{GeO}_2$  and  $\text{SiO}_2$  differ is in the distribution of tetrahedron bond angles. The bond angle  $\angle\text{O-Si-O}$  in silica glass is constrained to a narrow region, from  $108^\circ$  to  $111^\circ$  [21]. For this reason, ab initio calculations performed in our previous study [10] for the model cluster  $(\text{OH})_3\text{Si-O-Si}(\text{OH})_3$  considered only  $\angle\text{O-Si-O} \approx 109.5^\circ$ . For amorphous  $\text{GeO}_2$ , however, it has been suggested that a larger variation in the angle  $\angle\text{O-Ge-O}$  is present, with values ranging from  $104^\circ$  to  $115^\circ$  [20,21]. Accordingly, the six angles  $\angle\text{O-Ge-OH}$  in the model cluster examined in the present investigation were identically varied from  $105^\circ$  to  $115^\circ$ .

In both the eclipsed and staggered configurations the distances  $d(\text{Ge-O})$  and  $d(\text{O-H})$  (identical for all Ge, O and H) were optimized with the angles  $\angle\text{Ge-O-Ge}$  and  $\angle\text{O-Ge-OH}$  fixed using a

6-31 + G(d) basis set for oxygen and hydrogen and a 6-311 + G(d) basis set for germanium. For the staggered configuration, the angle  $\angle\text{O-Ge-OH}$  was also fixed at  $105^\circ$  or  $115^\circ$  and the distances  $d(\text{Ge-O})$  and  $d(\text{O-H})$  optimized. For the eclipsed configuration the angle  $\angle\text{O-Ge-OH}$  was fixed at  $109.5^\circ$ . The final parameters are listed in Table 1.

The relative energies of clusters with various structural parameters calculated with respect to that of a staggered cluster with the angle  $\angle\text{Ge-O-Ge}$  set to  $180^\circ$  are also included in Table 1. A plot showing the energy curves for clusters with staggered or eclipsed geometry as a function of the angle  $\angle\text{Ge-O-Ge}$  is shown in Fig. 2.

The dependence of the ab initio predicted  $^{17}\text{O}$   $C_q$  and  $\eta_q$  parameters for the bridging oxygen in the  $(\text{OH})_3\text{Ge-O-Ge}(\text{OH})_3$  cluster as a function of  $\text{Ge-O-Ge}$  bond angle are shown in Fig. 3 for clusters in which the angle  $\angle\text{O-Ge-OH}$  has been varied from  $105^\circ$  to  $115^\circ$ . The results reported for a silicate cluster have been included for comparison [10]. Also, the experimentally measured  $C_q$  and  $\eta_q$  value for the bridging oxygen in the  $\alpha$ -quartz form of  $\text{GeO}_2$  ( $\angle\text{Ge-O-Ge} = 130^\circ$ ) is indicated.

Finally, when comparing the structure of amorphous  $\text{GeO}_2$  and  $\text{SiO}_2$  it is apparent that the metal–oxygen distance in germanates is greater than that in silicates. The effect that this difference may have on the bridging oxygen quadrupole coupling parameters has been considered for clusters including Group IV elements carbon, silicon and germanium. A series of calculations have been performed (shown in Fig. 5) on a staggered  $(\text{OH})_3\text{X-O-X}(\text{OH})_3$  cluster with the angle  $\angle\text{X-O-X}$  held constant at  $180^\circ$  while independently varying both the distance  $d(\text{X-O})$  around their equilibrium bond lengths (shown as filled data points) and the nature of the coordinating cation, i.e.,  $\text{X} = \text{C}, \text{Si}$  and  $\text{Ge}$ .

### 4. Discussion

As seen in Table 1 the optimized distance  $d(\text{O-H})$  is dependent on the angle  $\angle\text{O-Ge-OH}$  while being independent of the angle  $\angle\text{Ge-O-Ge}$ . When the angle  $\angle\text{O-Ge-OH}$  is diminished,  $d(\text{O-H})$  increases systematically for all  $\angle\text{Ge-O-Ge}$ . The

Table 1

$^{17}\text{O}$  quadrupolar coupling parameters, distances and relative energies obtained from ab initio calculations on the  $(\text{OH})_3\text{Ge-O-Ge}(\text{OH})_3$  molecule in staggered and eclipsed configurations as a function of O–Ge–O and Ge–O–Ge angles. The Euler angles  $\alpha_q$ ,  $\beta_q$  and  $\gamma_q$ , which give the orientation of the EFG PAS with respect to a molecular frame with the x- and z-axes lying in the plane of the  $\angle\text{Ge-O-Ge}$  with the z-axis perpendicular to the bisector of the Ge–O–Ge angle (see Fig. 4), were identically zero at all Ge–O–Ge angles. The energies are referenced with respect to the staggered cluster with the angle  $\angle\text{Ge-O-Ge}$  set to  $180^\circ$

$\angle\text{Ge-O-Ge}$ ( $^\circ$ )	$\angle\text{O-Ge-OH}$ ( $^\circ$ )	Staggered					Eclipsed			
		$d(\text{Ge-O})$ ( $\text{\AA}$ )	$d(\text{OH})$ ( $\text{\AA}$ )	Energy (kJ/mol)	$C_q$ (MHz)	$\eta_q$	$d(\text{Ge-O})$ ( $\text{\AA}$ )	Energy (kJ/mol)	$C_q$ (MHz)	$\eta_q$
120	105.0	1.748	0.952	50.0	-6.43	0.76				
120	109.5	1.742	0.949	6.2	-6.50	0.84	1.747	42.19	-6.54	0.78
120	115.0	1.740	0.946	49.6	-6.75	0.84				
130	105.0	1.742	0.952	38.0	-7.18	0.49				
130	109.5	1.739	0.949	-4.4	-7.35	0.51	1.741	6.59	-7.26	0.48
130	115.0	1.737	0.946	39.6	-7.61	0.53				
140	105.0	1.742	0.952	36.2	-7.77	0.29				
140	109.5	1.737	0.949	-7.0	-7.99	0.31	1.738	-2.56	-7.97	0.29
140	115.0	1.735	0.946	34.7	-8.30	0.32				
150	105.0	1.740	0.952	36.6	-8.22	0.16				
150	109.5	1.736	0.949	-5.7	-8.47	0.17	1.736	-3.28	-8.46	0.15
150	115.0	1.734	0.946	38.7	-8.82	0.17				
160	105.0	1.739	0.952	39.1	-8.54	0.07				
160	109.5	1.734	0.949	-3.1	-8.81	0.07	1.734	-1.52	-8.80	0.06
160	115.0	1.732	0.946	41.4	-9.20	0.10				
170	105.0	1.738	0.952	41.3	-8.74	0.02				
170	109.5	1.734	0.949	-0.9	-9.03	0.02	1.734	0.34	-9.02	0.01
170	115.0	1.731	0.946	43.7	-9.43	0.02				
180	105.0	1.738	0.952	42.1	-8.81	0.00				
180	109.5	1.733	0.949	0.0	-9.10	0.00	1.733	1.10	-9.10	0.00
180	115.0	1.731	0.946	44.6	-9.51	0.00				

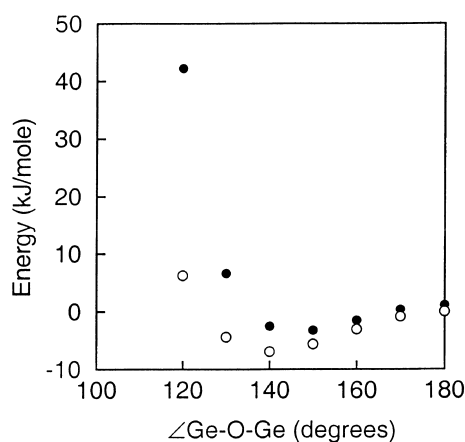


Fig. 2. Ab initio calculated values in energy as a function of Ge–O–Ge bond angle in  $(\text{OH})_3\text{Ge-O-Ge}(\text{OH})_3$  which has an O–Ge–O angle of  $109.5^\circ$ . Filled and open circles are the eclipsed and staggered configurations, respectively.

$d(\text{Ge-O})$  distance is, however, dependent on the angle  $\angle\text{Ge-O-Ge}$ . The optimized geometry of the  $(\text{OH})_3\text{Ge-O-Ge}(\text{OH})_3$  cluster demonstrates a trend of decreasing  $d(\text{Ge-O})$  as the angle  $\angle\text{Ge-O-Ge}$  increases and this trend in interatomic distance is similar to that calculated for the cluster  $(\text{OH})_3\text{Si-O-Si}(\text{OH})_3$  [10]. The distance  $d(\text{Ge-O})$  is significantly longer than the computed distance  $d(\text{Si-O})$  which ranged from 1.647 to 1.632  $\text{\AA}$  as the angle  $\angle\text{Si-O-Si}$  increased from  $120^\circ$  to  $180^\circ$  [8,10,22]. These computed values are in agreement with experimental results; the mean Ge–O distance in  $\text{GeO}_2$  glass is approximately 1.739  $\text{\AA}$  [20], while the mean Si–O distance in  $\text{SiO}_2$  is 1.62  $\text{\AA}$  [23].

The energy minima of the  $(\text{OH})_3\text{Ge-O-Ge}(\text{OH})_3$  cluster as a function of the angle  $\angle\text{Ge-O-Ge}$  shown in Fig. 2 indicate that the lowest energy

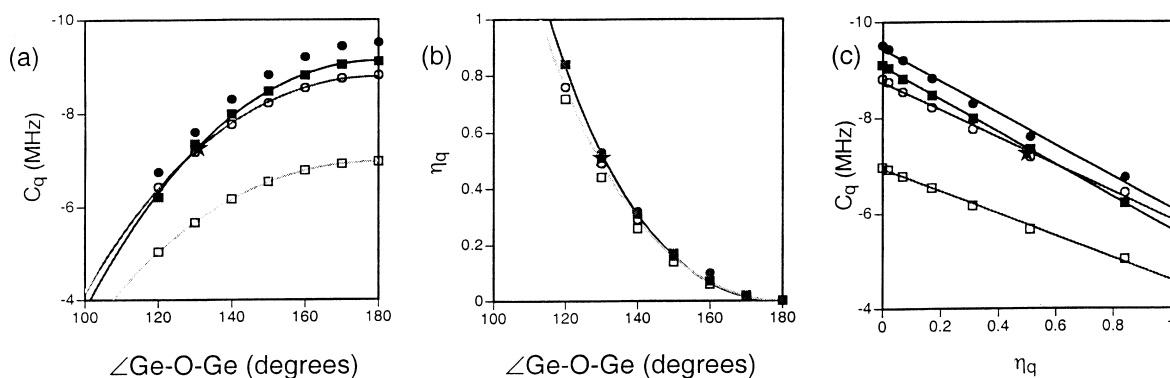


Fig. 3. Ab initio predicted values in (a)  $^{17}\text{O}$  quadrupolar coupling constant,  $C_q$ , (b) the  $^{17}\text{O}$  quadrupolar asymmetry parameter,  $\eta_q$  and (c) the correlation between  $C_q$  and  $\eta_q$  as a function of bridging oxygen angle and the angle  $\angle\text{O-Ge-OH}$  in the cluster  $(\text{OH})_3\text{Ge-O-Ge}(\text{OH})_3$  with a staggered configuration. The values for  $(\text{OH})_3\text{Ge-O-Ge}(\text{OH})_3$  are calculated with angles  $\angle\text{O-Ge-OH}$  of  $105^\circ$ ,  $109.5^\circ$ , and  $115^\circ$ , shown as the open circles, filled squares and filled circles, respectively. The solid lines represents the best fit of Eq. (2). For comparison, the ab initio predicted values [10] for the cluster  $(\text{OH})_3\text{Si-O-Si}(\text{OH})_3$  are shown as the open squares. The experimentally measured  $C_q$  and  $\eta_q$  value for the bridging oxygen in the  $\alpha$ -quartz form of  $\text{GeO}_2$  ( $\angle\text{Ge-O-Ge} = 130^\circ$ ) is indicated in all three plots by a filled star.

configuration for this model cluster is a staggered configuration with a bridging angle  $\angle\text{Ge-O-Ge}$  of  $140^\circ$ . Although this result is in reasonable agreement with experimental data which suggest an average bridging angle of  $133^\circ$  for amorphous  $\text{GeO}_2$  [18,20], such agreement is perhaps fortuitous. The experimentally determined range of  $\angle\text{Ge-O-Ge}$  in amorphous  $\text{GeO}_2$  has a narrow distribution of approximately  $10^\circ$  (in comparison to a range of  $120$ – $180^\circ$  in amorphous  $\text{SiO}_2$ ) [23]. However, the calculated change in energy in the  $(\text{OH})_3\text{Ge-O-Ge}(\text{OH})_3$  model cluster between the staggered configuration with a bridging angle of  $130^\circ$  and the eclipsed configuration with a bridging angle of  $180^\circ$  is only  $5.5$  kJ/mol. This result suggests that higher coordination sphere structures, such as rings, may have a significant influence on stabilizing structures which result in a bridging angle near  $133^\circ$ . This is in agreement with models of vitreous  $\text{GeO}_2$  which suggest that medium range order in the  $\text{GeO}_2$  network is dominated by the presence of ring structures, including a large population of three-member rings which have a  $\text{Ge-O-Ge}$  angle of  $130.5^\circ$  [24,25].

When the angle  $\angle\text{O-Ge-O}$  is varied from its experimentally determined mean value of approximately  $109.5^\circ$  the resulting model cluster geometries are energetically less favorable (see Table 1).

For example, a variation in the angle  $\angle\text{O-Ge-OH}$  by  $5^\circ$  results in an increase in energy of approximately  $40$  kJ/mol. In light of this large energy barrier, the proposed existence of such variations in vitreous  $\text{GeO}_2$  also requires the existence of higher coordination sphere structures which could stabilize an  $\angle\text{O-Ge-O}$  distribution between the reported values of  $104$ – $115^\circ$ .

The dependence of the ab initio predicted  $^{17}\text{O}$   $C_q$  and  $\eta_q$  parameters for the bridging oxygen in the  $(\text{OH})_3\text{Ge-O-Ge}(\text{OH})_3$  cluster as a function of  $\text{Ge-O-Ge}$  bond angle when the six angles  $\angle\text{O-Ge-OH}$  in the model cluster were identically varied from  $105^\circ$  to  $115^\circ$  are shown in Fig. 3. The trends are similar to those reported for the comparable silicate cluster [7,26,27]. Over the range of expected  $\angle\text{O-Ge-O}$  values, the  $C_q$  parameter varies by greater than  $0.3$  MHz while the  $\eta_q$  parameter varies noticeably only at the lower  $\text{Ge-O-Ge}$  angles. This change in the  $C_q$  parameter may be attributed to variations in both the  $d(\text{Ge-O})$  value and in Ge hybridization, both of which are related to the angle  $\angle\text{O-Ge-OH}$ . If a wide distribution of  $\text{O-Ge-O}$  angles are present in a structure then this variability in  $C_q$  could mitigate the effectiveness of this parameter as a probe of  $\text{Ge-O-Ge}$  angle. However, the relative invariance in  $\eta_q$  as a function of the angle  $\angle\text{O-Ge-OH}$  suggests that  $\eta_q$  may still

provide information regarding the Ge–O–Ge angle. In all cases considered the orientation of the bridging oxygen EFG principal axis system (PAS) in the germanate cluster (shown in Fig. 4) is the same as that for the silicate cluster. The EFG PAS has its  $x$ - and  $z$ -axes lying in the plane of the Ge–O–Ge angle, with the  $z$ -axis perpendicular to the bisector of the Ge–O–Ge angle. Variability in the angle  $\angle\text{O–Ge–O}$  did not affect the EFG PAS for the germanate cluster.

In general, the magnitude of *ab initio* predicted EFG tensor eigenvalues need to be calibrated with experimental values. Unfortunately, little  $^{17}\text{O}$  experimental data exist with which to confirm these *ab initio* results. One system which has been investigated [11,12] is  $\alpha$ -quartz, which has a Ge–O–Ge angle of  $130^\circ$  [21] and an O–Ge–O angle of  $107$ – $112^\circ$  [21]. The NMR parameters for  $\alpha$ -quartz, as determined experimentally by MAS are  $|C_q| = 7.3$  MHz and  $\eta_q = 0.48$ . These results are shown along with the predicted *ab initio* values for  $C_q$  and  $\eta_q$  in Fig. 3 and appear to be in excellent agreement with calculated values for a comparable germanate model cluster with a Ge–O–Ge angle of  $130^\circ$ . Thus based on this one measurement we tentatively conclude that there is no need to shift the EFG tensor eigenvalues to calibrate the data.

While identical trends in  $C_q$  with bridging oxygen angle were observed for the silicate model cluster [10], the  $C_q$  values are systematically shifted higher in magnitude for the germanate cluster as shown in Fig. 3. There are two possible factors that could contribute to this shift in  $C_q$ . One is the dependence of  $C_q$  on the distance between the bridging oxygen and coordinating cation(s), i.e.,  $d(\text{Ge–O})$  vs.  $d(\text{Si–O})$  and the other is the depen-

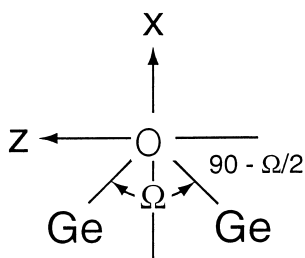


Fig. 4. Orientation of the EFG tensor with respect to the Ge–O–Ge molecular frame.

dence of  $C_q$  on the electronegativity of the coordinating cation. The relationship between bond covalency and the  $C_q$  parameter for crystalline compounds has been investigated earlier [28,29] with an increase in bond covalency corresponding to an increase in the magnitude of the  $C_q$  parameter. Based on electronegativity differences alone one would predict that the  $C_q$  parameter for the germanate cluster will be greater than that of the silicate cluster, while being smaller than those for clusters containing more electronegative coordinating cations such as carbon.

To determine the relative size of these two effects we performed a series of calculations (shown in Fig. 5) on a staggered  $(\text{OH})_3\text{X–O–X}(\text{OH})_3$  cluster with the angle  $\angle\text{X–O–X}$  held constant at  $180^\circ$  and independently varied both the distance  $d(\text{X–O})$  around their equilibrium bond lengths (shown as filled data points) and the nature of the coordinating cation, i.e.,  $\text{X} = \text{C}, \text{Si}$  and  $\text{Ge}$ .

Clearly there is a strong correlation between  $C_q$  and both  $d(\text{X–O})$  and coordinating cation electronegativity, with both increasing distance  $d(\text{X–O})$  and increasing electronegativity resulting in increased magnitudes of  $C_q$ . In the case of the

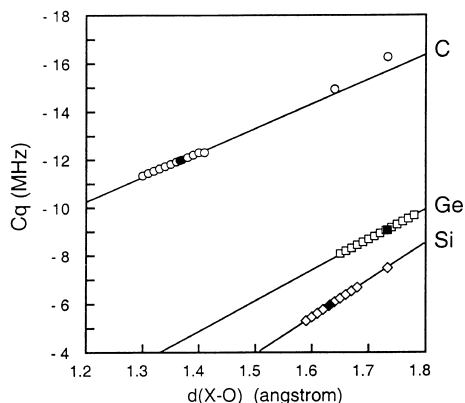


Fig. 5. Comparison of bridging oxygen  $^{17}\text{O}$   $C_q$  values for the clusters  $(\text{OH})_3\text{X–O–X}(\text{OH})_3$ , where  $\text{X} = \text{C}$  (represented by open circles),  $\text{Si}$  (open diamonds) and  $\text{Ge}$  (open squares) as a function of  $d(\text{X–O})$ . In all calculations the angle  $\angle\text{X–O–X}$  was held fixed at  $180^\circ$  and the optimized  $d(\text{X–O})$  values for this angle are represented by filled symbols. The *ab initio* calculated results for the carbon and silicon clusters have been decreased in magnitude by 4 and 1 MHz, respectively, to be in agreement with experimental results [28,29].

germanate cluster the systematic shift in  $C_q$  in comparison to the silicate cluster arises approximately equally from both the difference in the equilibrium distance  $d(X-O)$  and the electronegativity difference. Although the effect of the shorter distance  $d(C-O)$  in the optimized cluster  $(OH)_3C-O-C(OH)_3$  is to reduce the magnitude of  $C_q$  there still remains a substantial increase in the magnitude of  $C_q$  in the optimized cluster due to the higher electronegativity of carbon.

It has been suggested that  $SnO_4$  and  $PbO_4$  structures are present in modified silicate environments [30–32]. If such bridging oxygen sites do exist then the magnitude of the  $C_q$  for a bridging oxygen atom connecting these sites would be expected to be even greater than that for analogous silicate or germanate clusters on the basis of both electronegativities and coordinating cation–oxygen distances. Finally, it is also interesting to note that with all the Group IV elements the magnitude of  $C_q$  for the bridging oxygen is lowest when coordinated by silicon.

In an earlier work [27], we used the semi-empirical Townes–Dailey theory [33] to obtain the analytical expressions for  $C_q$  and  $\eta_q$  as a function of bridging oxygen angle. Recently, we modified these expressions to a more generic form

$$C_q(\Omega) = a \left( \frac{1}{2} + \frac{\cos \Omega}{\cos \Omega - 1} \right)^\alpha, \quad (2)$$

$$\eta_q(\Omega) = b \left( \frac{1}{2} - \frac{\cos \Omega}{\cos \Omega - 1} \right)^\beta,$$

which gives better agreement with the ab initio and experimental data with  $\alpha$  values near 2. When applied to the ab initio data given in Table 1 we obtain the best-fit parameters given in Table 2. The best-fit curves using these parameters are also shown in Fig. 3. The parameter  $a$  in our  $C_q$  expression ranged from  $-8.78$  to  $-9.48$  MHz for

$\angle O-Ge-O = 105-115^\circ$ , respectively, with an approximately linear relationship existing between the parameter  $a$  and the angle  $\angle O-Ge-O$ . The parameter  $b$  in our expression for  $\eta_q$  ranged from 4.76 to 5.69 for  $\angle O-Ge-O = 105^\circ-115^\circ$ , respectively.

Using the relationships obtained in this work we have re-examined the recent  $^{17}O$  results of Hussin et al. [12], where a distribution of  $C_q$  values having a mean of 7.1 MHz and a full width at half maximum (FWHM) of 0.7 MHz and a distribution of  $\eta_q$  values having a mean of 0.48 and a FWHM of 0.18 were obtained. Based on the results presented herein these  $C_q$  values correspond to a mean  $\angle Ge-O-Ge$  of  $128.5^\circ$  and assuming a symmetric distribution of  $C_q$  values, the FWHM corresponds to a  $8.3^\circ$  spread in  $Ge-O-Ge$  angles. Similarly, the  $\eta_q$  values correspond to a mean  $\angle Ge-O-Ge$  of  $132.0^\circ$  and again assuming a symmetric distribution of  $\eta_q$  values, the FWHM corresponds to a  $7.4^\circ$  spread in  $Ge-O-Ge$  angles. These results are in close agreement with those obtained by Hussin et al. and again suggest a significantly narrower distribution in bridging oxygen angles in  $GeO_2$  glass in comparison to  $SiO_2$  glass.

## 5. Conclusions

Based on our ab initio calculations, relationships between  $^{17}O$  quadrupolar coupling parameters and the local structure around the bridging oxygen in the model cluster  $(OH)_3Ge-O-Ge(OH)_3$  are predicted to be similar to those previously reported for bridging oxygen in silicate model clusters. A systematic increase in the  $^{17}O$   $C_q$  of approximately 3 MHz was found for the germanate bridging oxygen in comparison to the silicate model clusters. This shift arises approximately equally from both the difference in dis-

Table 2  
Best fit parameters of Eqs. (2) to the ab initio predicted  $C_q$  and  $\eta_q$  data

$\angle Ge-O-Ge$ ( $^\circ$ )	Staggered				Eclipsed			
	$a$ (MHz)	$\alpha$	$b$	$\beta$	$a$ (MHz)	$\alpha$	$b$	$\beta$
105.0	-8.78	1.73	4.76	1.02				
109.5	-9.12	2.02	5.69	1.07	-9.07	1.85	5.42	1.08
115.0	-9.48	1.89	5.19	1.02				

tances  $d(\text{Ge-O})$  and  $d(\text{Si-O})$  and the differences in Ge and Si electronegativity.

Germanate tetrahedra are also thought to undergo greater distortions of the intratetrahedron bond angles in comparison to silicate tetrahedra. We find that  $C_q$  is weakly correlated to these distortions and thus its effectiveness as a probe of Ge–O–Ge angle is somewhat mitigated. In contrast, however,  $\eta_q$  is insensitive to such distortions and can still serve as a reliable probe of Ge–O–Ge angle. Thus, a measure of both  $C_q$  and  $\eta_q$  could be effectively used to measure both the Ge–O–Ge angle and the degree of intratetrahedron bond angle distortions.

### Acknowledgements

This work was supported by a grant from the National Science Foundation (No. CHE-9807498).

### References

- [1] A. Llor, J. Virlet, Chem. Phys. Lett. 152 (1988) 248.
- [2] B.F. Chmelka, K.T. Mueller, A. Pines, J. Stebbins, Y. Wu, J.W. Zwanziger, Nature 339 (1989) 42.
- [3] L. Frydman, J.S. Harwood, J. Am. Chem. Soc. 117 (1995) 5367.
- [4] I. Farnan, P.J. Grandinetti, J.H. Baltisberger, J.F. Stebbins, U. Werner, M.A. Eastman, A. Pines, Nature 358 (1992) 31.
- [5] S. Kuroki, A. Takahashi, I. Ando, A. Shoji, T. Ozaki, J. Mol. Struct. 323 (1994) 197.
- [6] R.K. Harris, M.J. Leach, D.P. Thompson, Chem. Mater. 4 (2) (1992) 260.
- [7] J.A. Tossell, P. Lazzarotti, Chem. Phys. Lett. 112 (1987) 205.
- [8] K.L. Geisinger, G.V. Gibbs, A. Navrotsky, Phys. Chem. Minerals 11 (1985) 266.
- [9] L.A. Curtiss, M.P. McGrath, J.P. Blaudeau, N.E. Davis, R.C. Binning, L. Random, J. Chem. Phys. 103 (14) (1995) 6104.
- [10] K.E. Vermillion, P. Florian, P.J. Grandinetti, J. Chem. Phys. 108 (17) (1998) 7274.
- [11] R. Hussin, D. Holland, R. Dupree, J. Non-Cryst. Solids 234 (1998) 440.
- [12] R. Hussin, R. Dupree, D. Holland, J. Non-Cryst. Solids 246 (3) (1999) 159.
- [13] M.J. Frisch, G.W. Trucks, H.B. Schlegel, P.M.W. Gill, B.G. Johnson, M.A. Robb, J.R. Cheeseman, T. Keith, G.A. Petersson, J.A. Montgomery, K. Raghavachari, M.A. Al-Laham, V.G. Zakrzewski, J.V. Ortiz, J.B. Foresman, C.Y. Peng, P.Y. Ayala, W. Chen, M.W. Wong, J.L. Andres, E.S. Replogle, R. Comperts, R.L. Martin, D.J. Fox, J.S. Binkley, D.J. Defrees, J. Baker, J.P. Stewart, M. Head-Gordon, C. Gonzalez, J.A. Pople, Gaussian '94, revision b.3. Gaussian, Inc., Pittsburgh PA, 1995.
- [14] Y. Yashiro, A. Yoshiasa, O. Kamishima, T. Tsuchiya, T. Yamanaka, T. Ishii, H. Maeda, J. Phys. (Paris) IV 7 (C2) (1997) 1175.
- [15] M. Okuno, C.D. Yin, H. Morikawa, F. Marumo, J. Non-Cryst. Solids 87 (1986) 312.
- [16] G.S. Henderson, M.E. Fleet, J. Non-Cryst. Solids 134 (1991) 259.
- [17] D.J. Durben, G. Wolf, Phys. Rev. B 43 (1991) 2355.
- [18] A.J. Leadbetter, A.C. Wright, J. Non-Cryst. Solids 7 (1972) 37.
- [19] P. Bondot, Phys. Status Solid A 22 (1974) 511.
- [20] A.C. Wright, J.A.E. Desa, R.N. Sinclair, J. Non-Cryst. Solids 99 (1988) 276.
- [21] J.D. Jorgensen, J. Appl. Phys. 49 (1978) 5473.
- [22] G.V. Gibbs, Am. Miner. 67 (1982) 421.
- [23] R.L. Mozzi, B.E. Warren, J. Appl. Crystallogr. 2 (1969) 164.
- [24] A.S. Zyubin, O.A. Kondakova, S.A. Dembovsky, Glass Phys. Chem. 23 (1997) 58.
- [25] F.L. Galeener, Solid State Commun. 44 (1982) 1037.
- [26] C.G. Lindsay, J.A. Tossell, Phys. Chem. Minerals 18 (1991) 191.
- [27] P.J. Grandinetti, J.H. Baltisberger, U. Werner, A. Pines, I. Farnan, J.F. Stebbins, J. Phys. Chem. 99 (1995) 12341.
- [28] H.K. Timkin, PhD thesis, University of Illinois, Urbana-Champaign, 1986.
- [29] S. Schramm, E. Oldfield, J. Am. Chem. Soc. 106 (1984) 2502.
- [30] J.F. Bent, A.C. Hannon, D. Holland, M.M.A. Karim, J. Non-Cryst. Solids 232–234 (1998) 300.
- [31] F. Fayon, C. Bessada, D. Massiot, I. Farnan, J.P. Couettes, J. Non-Cryst. Solids 232–234 (1998) 403.
- [32] F. Fayon, C. Landron, K. Sakurai, C. Bessada, D. Massiot, J. Non-Cryst. Solids 243 (1999) 39.
- [33] C.H. Townes, B.P. Dailey, J. Chem. Phys. 17 (1949) 782.